Electronic Supplementary Information

Enhanced Reversibility and Durability of Solid Oxide Fe-air Redox Battery by Carbothermic Reaction Derived Energy Storage Materials

Xuan Zhao, Xue Li, Yunhui Gong, Kevin Huang*

Department of Mechanical Engineering, University of South Carolina, SC, 29201

Carbothermic synthesis of Fe-based redox couple (Fe/C)

The starting materials for the reaction are a co-precipitated Fe_2O_3-ZrO_2 powder and carbon black (Fisher Scientific). The two powders were first intimately mixed in an atomic ratio of Fe:C=1:4.2, followed by ball milling in alcohol. The excess stoichiometry of C was intentional to ensure a full reduction of Fe_2O_3 to Fe. The mixed/milled powders were dried, and pressed into pellets. The pellets were then reacted at 1000^{o}C for 10 h in flowing N_2 at 100 sccm. The final product contains Fe/C/ZrO_2 as verified by XRD and SEM/EDS shown in the main manuscript.

The iron carbothermic reaction can be described as follows:

$$C + Fe_2O_3 = Fe + CO_2 \quad \text{(S-1)}$$

$$CO_2 + C = 2CO \quad \text{(S-2)}$$

An Ellingham diagram is constructed from thermodynamic data and shown in Fig.S1. It is evident that a temperature above 750°C would lead to a full reaction of carbon with iron oxides, resulting in metallic iron. The reaction temperature of 1000°C employed in this study is sufficiently high to reduce iron oxide into metallic iron by carbon. In addition to the solid products, CO and CO_2 are the gaseous products constantly removed by the carrier gas N_2 during the reaction.

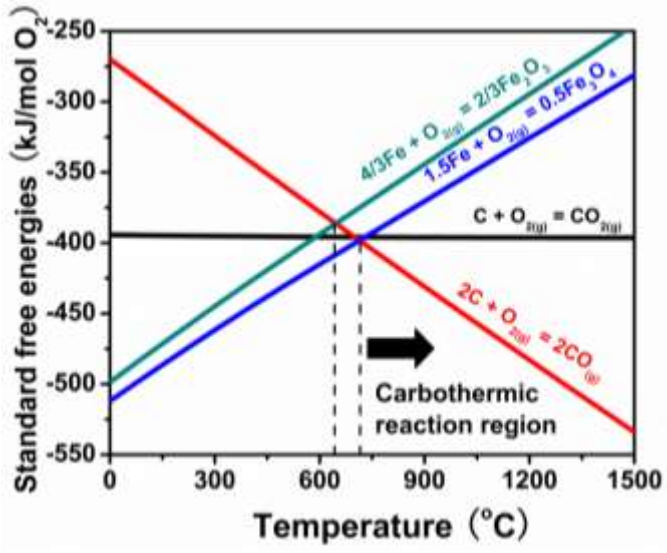

Fig.S1 Ellingham diagram of Fe-C-O system

Battery assembly and testing

A simple planar button cell configuration was used for the battery test [1]. The RSOFC consisted of a tape-casted Sr- and Mg-doped $LaGaO_3$ (LSGM) electrolyte, a porous LSGM-supported $Sm_{0.5}Sr_{0.5}CoO_{3-\delta}$ (SSC)-$Sm_{0.2}Ce_{0.8}O_{1.9}$ (SDC) air-electrode prepared by infiltration of nitrate solutions [2], and a Ni-CeO_2 cermet fuel-electrode, all homemade in our lab. The cell's active surface area was 1.3 cm^2.

At the beginning of each test, the Fe/C ESM was first exposed to a mixture of 5% H_2-N_2 to

protect the metallic iron during the ramping up to 650^{o}C, at which the glass sealant was melted. After roughly 30 minutes, 5%H_2-N_2 was switched to pure H_2, followed by ramping down to the testing temperature of 550^{o}C. The use of pure H_2 was to create the wanted Fe-Fe_3O_4 redox couple by applying a small discharge current from the RSOFC. The battery's EMF was constantly monitored during the discharge process to prevent over-oxidation of the Fe. As soon as the EMF reached 1.07 volts, the theoretical Nernst potential for the Fe-Fe_3O_4 equilibrium at 550^{o}C, the electrochemical oxidation was stopped and the system was ready for the discharge-and-charge cycles.

A Solartron 1260/1287 Electrochemical System was employed to characterize the electrical performance of the battery under various operating conditions with software modules such as OCV-t, impedance spectroscopy, and galvanic cycles.

Other characterizations

The microstructures and compositions of the RSOFC and Fe/C ESM before and after tests were examined with a field-emission scanning electron microscope (FESEM, Zeiss Ultra) equipped with EDX. The sample was specially treated to prevent attraction of particles to the SEM lens. The surface areas and porosities of the Fe/C ESM before and after tests were analyzed by a Micromeritics ASAP 2020 -Surface Area Analyzer and Autopore IV Porosimeter, respectively. The phase purity of the ESM were also examined by powder X-ray diffraction (PXRD) with an X-ray diffractometer (D/max-A, Rigaku, Japan) and graphite-monochromatized CuKα radiation (λ=1.5418 Å). The XRD scan was performed at a rate of 5^{o} min^{-1} from 2θ= 10^{o} to 90^{o}, the spectrum of which was analyzed with the JADE (MDI)

software to identify phase compositions.

To determine the carbon contents in a Fe/C-ESM, either as-synthesized or tested, a simple chemical analysis method was used. The sample was first weighed and then soaked in a diluted nitric acid (20 vol%) in a beaker. After approximately one week, all the Fe was completely dissolved in the acid; only ZrO_2 and C were left on the bottom of the beaker. After a thorough rinsing with DI water, the residual solids were dried and weighed again. Since the ratio between Zr and Fe was previously known, the content of C in the original sample could then be easily calculated out. The determined C content in the as-synthesized Fe/C-ESM was 37%. After test, there was roughly 15% C loss in the ESM. A thermodynamic analysis of the equilibrium compositions of the system seems to support the observation. Fig.S2 shows that gasification of C into CO and CO_2 could occur above 450°C even though the magnitude of the reaction is small.

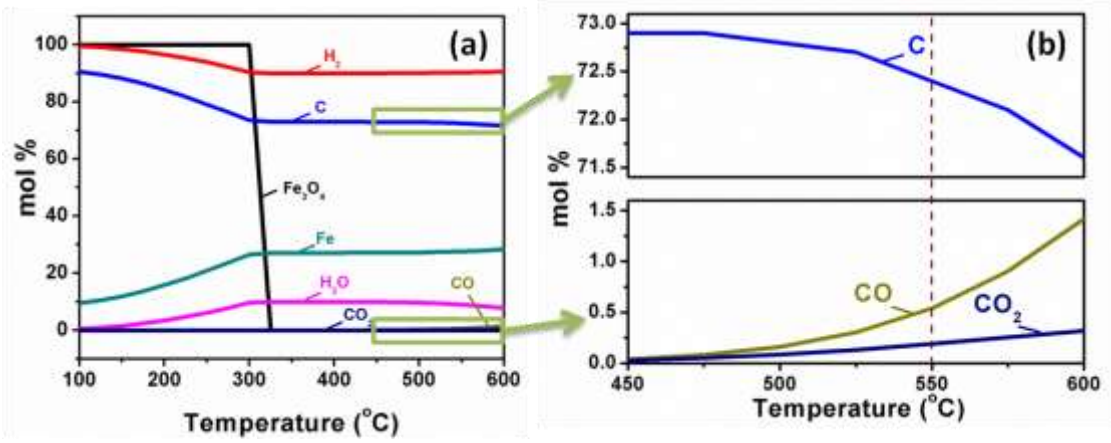

Fig.S2 Equilibrium compositions as a function of temperatures of (a) all the relevant components and (b) carbon-related components in a simulated environment to the Fe/C-air battery

Electrochemical Impedance Spectroscopy (EIS)

To investigate the root causes for the performance difference observed in the Fe/C-air and Fe-air batteries, we studied the EIS spectra from both batteries before and after 100th cycles. Fig.S3 shows that impedance spectra of the two batteries prior to cyclic testing are similar. It is not surprising that they used exactly the same type of RSOFCs. After the 100-cycle, however, the total ASR (area specific resistance) of the RSOFC with Fe/C-ESM increased by 11.5 Ω·cm^2, much less than 44.5 Ω·cm^2 found for the Fe ESM. After reduction by H_2, both RSOFCs showed signs of recovery, but only the RSOFC with Fe/C ESM restored close to its initial performance. The ASR of RSOFC with Fe ESM was ~22 Ωcm^2, nearly twice the initial value. These comparisons suggest that the ESM has an effect on the performance of RSOFC. Faster redox kinetics and better oxygen shuttling action between ESM and RSOFC can support a faster mass transfer and charge transfer in the fuel electrode of the RSOFC.

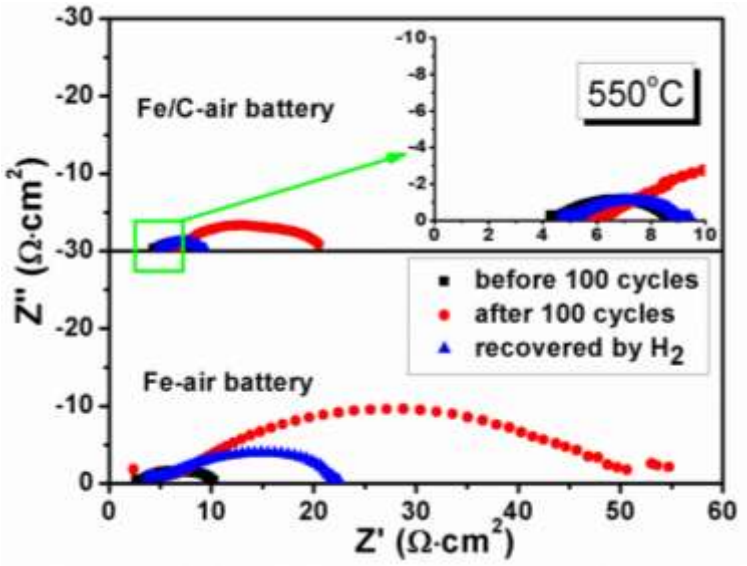

Fig.S3 Comparison of EIS spectra measured from the baseline Fe-air and Fe/C-air batteries under different states.

Microstructures of the post-test ESM

The microstructure of Fe/C ESM after test is shown in Fig.S4. Compositionally, there seems to be no significant difference between the darker and lighter particles (zone-1 vs zone-2), but carbon is clearly observed to concentrate on the surface (zone-3). The BET surface area of this post-test Fe/C-ESM is 10.5m^2/g, slightly smaller than the initial value 12.5m^2/g, suggesting little agglomeration of Fe-particles occurred during the battery test.

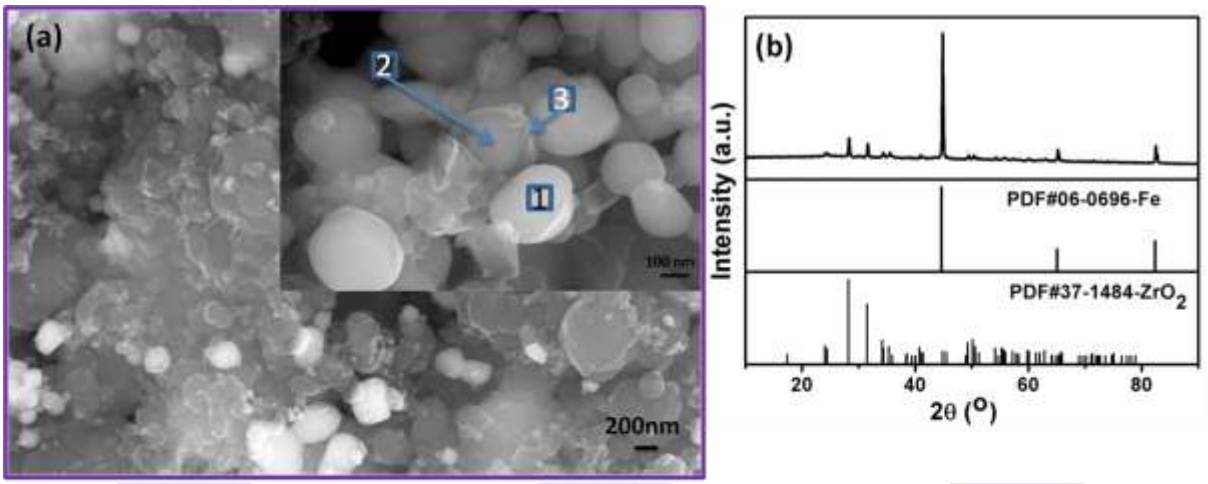

Zone 1

Element	Wt%	At%
C K	41.46	62.14
O K	25.83	29.07
Zr L	14.01	2.76
Fe K	18.70	6.03
Total	100	100

Zone 2

Element	Wt%	At%
C K	41.48	62.54
O K	25.06	28.37
Zr L	14.04	2.79
Fe K	19.42	6.30
Total	100	100

Zone 3

Element	Wt%	At%
C K	54.41	82.44
O K	5.62	6.39
Zr L	14.66	2.93
Fe K	25.30	8.25
Total	100	100

Fig.S4 Microstructure and composition of the post-test Fe/C-ESM: (a) morphology and (b) XRD pattern.

Microstructures of the post-test RSOFCs

The microstructures of the post-test RSOFC in the Fe/C-air battery are shown in Fig.S5, in which (a) depicts the three functional layers: air-electrode, electrolyte and fuel-electrode. The contacts between electrolyte and electrodes are continuous and intact. Fig.S5 (b) further shows that the bonding between air electrode and electrolyte was not affected after the 100 cycles, and the infiltrated SSC-SDC fine particles remain well dispersed in the porous LSGM skeleton after the test. Such an air-electrode structure is deemed beneficial to the retention of the battery's performance. Fig.S5 (c) shows that the bonding between fuel electrode and electrolyte was not affected either. This feature is different from what was observed in an Fe-air battery tested for 100 cycles at 650^{o}C where there was clearly a detachment between fuel-electrode and electrolyte [3]. Fig.S5 (d) shows that the double-layer anode still maintains a good porous structure with no detachment discerned.

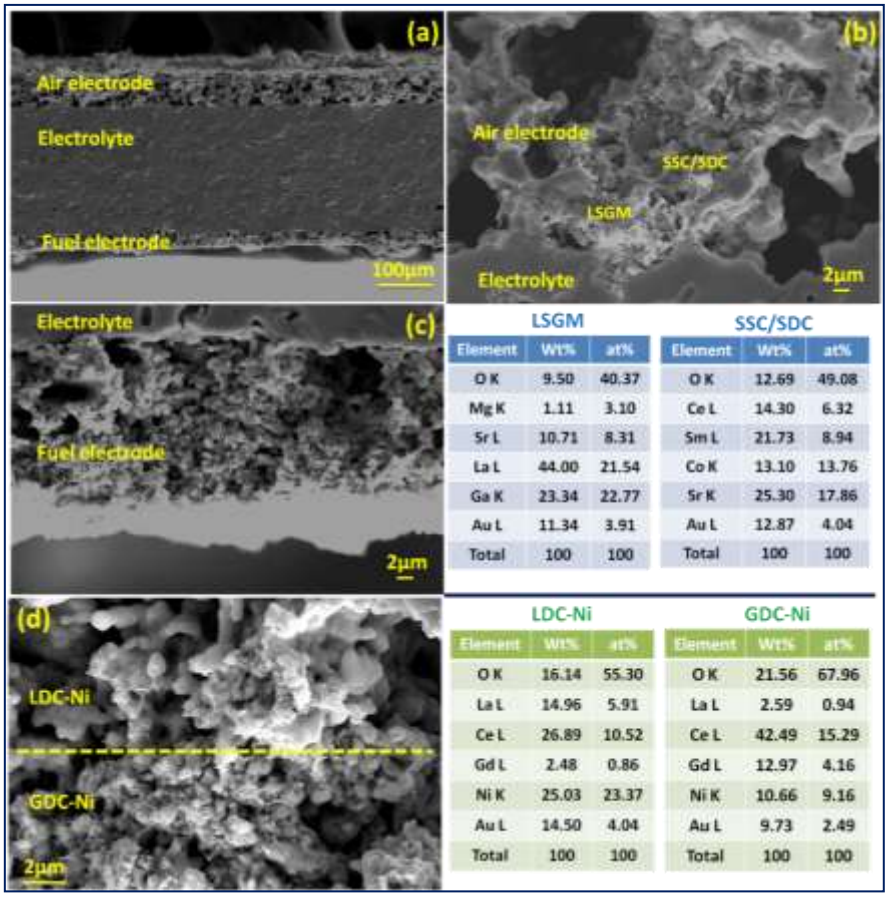

LSGM

Element	Wt%	at%
O K	9.50	40.37
Mg K	1.11	3.10
Sr L	10.71	8.31
La L	44.00	21.54
Ga K	23.34	22.77
Au L	11.34	3.91
Total	100	100

SSC/SDC

Element	Wt%	at%
O K	12.69	49.08
Ce L	14.30	6.32
Sm L	21.73	8.94
Co K	13.10	13.76
Sr K	25.30	17.86
Au L	12.87	4.04
Total	100	100

LDC-Ni

Element	Wt%	at%
O K	16.14	55.30
La L	14.96	5.91
Ce L	26.89	10.52
Gd L	2.48	0.86
Ni K	25.03	23.37
Au L	14.50	4.04
Total	100	100

GDC-Ni

Element	Wt%	at%
O K	21.56	67.96
La L	2.59	0.94
Ce L	42.49	15.29
Gd L	12.97	4.16
Ni K	10.66	9.16
Au L	9.73	2.49
Total	100	100

Fig.S5 Cross-sectional view of the microstructures and compositional analysis of the post-test RSOFC in the Fe/C-air battery: (a) whole battery; (b) electrolyte/air-electrode interface; (c) current collector/fuel-electrode/electrolyte interface; (d) fuel electrode with LDC-Ni and GDC-Ni dual layers (Note: the compositions given represent the highlighted zones).

References

[1] X. Zhao, Y. Gong, X. Li, N. Xu, K. Huang, *J. Electrochem. Soc.*, **160** (2013) A1241-A1247.

[2] Z. Zhan, D. Han, T. Wu, X. Ye, S. Wang, T. Wen, S. Cho, S.A. Barnett, *RSC Adv.*, **2** (2012) 4075-4078.

[3] X. Zhao, Y. Gong, X. Li, N. Xu, K. Huang, *J. Electrochem. Soc.*, **160** (2013) A1716-A1719.